

# Experimental testing of a horizontal-axis wind turbine to assess its performance

Filippo Spertino<sup>1</sup>, Alessandro Ciocia<sup>1</sup>, Paolo Di Leo<sup>1</sup>, Gaetano Iuso<sup>2</sup>, Gabriele Malgaroli<sup>1</sup>,  
Luca Roberto<sup>1</sup>

<sup>1</sup>*Politecnico di Torino, Dip. Energia, Torino, Italy, filippo.spertino@polito.it*

<sup>2</sup>*Politecnico di Torino, Dip. Ingegneria Meccanica e Aerospaziale, Torino, Italy, gaetano.iuso@polito.it*

**Abstract** – This paper describes a test procedure to investigate the performance of a micro wind turbine with horizontal-axis. A 3D model of a rotor with five blades has been designed by a MATLAB software; its airfoil is optimized to efficiently work at low wind speed. The rotor is coupled to an electric generator and this equipment is tested in a wind tunnel. An anemometer is used to measure and set the desired wind speeds. Electric quantities, i.e., voltage, current and power, are acquired by a digital multimeter. A variable resistance is used to change the operating point of the generator. Preliminary results are reported that refer to the application of the proposed test procedures to a wind turbine with a 0.2 m<sup>2</sup> swept area.

**Keywords** – Wind energy, electric variables measurement, uncertainty, data acquisition

## I. INTRODUCTION

The critical point in the operation of micro wind turbines is the coupling with an adequate commercial electrical generator. Actually, micro commercial generators are generally designed to efficiently work at high rotational speed (some thousands of revolutions per minute). A bladed rotor, designed to work at low speed, cannot achieve its maximum performance, when coupled with this kind of commercial generator. In case of high power wind turbines, a gearbox converts the low rotor speed into a high-speed [1]. Nevertheless, in case of micro scale wind generators, it is not an efficient and cost-effective solution.

This paper proposes a test procedure in order to quantify the performance of micro wind generators, with good accuracy. The procedure has been applied to a micro wind turbine with horizontal axis. Its airfoil is optimized by a MATLAB software to efficiently work at low speed; then, a prototype is built by a 3D printer. The turbine is characterized by a rotor with five blades and a swept area of 0.2 m<sup>2</sup>. The Betz's law [2] sets a threshold for the conversion of wind energy into mechanical

energy.



Fig. 1. The 3D model of the wind rotor under test

The coefficient of power is the appropriate parameter with a maximum value of 0.593. According to the mentioned Betz's law, at standard sea level (15 °C, 101.3 kPa), the theoretical maximum power of this device is  $P_{Betz} \approx 250$  W at a wind speed of 15 m/s. The rotor is directly coupled to a permanent magnet synchronous generator (PMSG) with rated power of 400 VA and speed of 3000 rpm. The 3D model of the rotor with five blades is shown in Fig. 1.

## II. DESCRIPTION OF THE PROCEDURE

The procedure for the measurement of wind turbine performance is carried out as follows.

First, the wind turbine is placed in a wind tunnel and the incident wind speed is regulated and set at the desired value. Then, the mechanical energy produced by the blades drives the PMSG. It supplies a resistive load, in which the resistance is changed to obtain different working points, starting from open-circuit condition. The physical quantities under measurement are: the wind speed  $U_{wind}$ , the rotor speed  $\omega$ , voltage  $V$  and current  $I$ . Data are stored in a Personal Computer (PC) and then elaborated.

The wind power  $P_{wind}$  (W) is a cubic function of the wind speed  $U_{wind}$  and is a quadratic function of the blade

length (here defined radius  $R$  of the rotor), assuming the standard air density  $\rho_{air}=1.225 \text{ kg/m}^3$ . To compare the performance of different wind turbines, it is advisable to define their global efficiency in terms of aerodynamic and electrical conversions, according to [3].

$$P_{wind} = \frac{1}{2} \rho_{air} \pi \cdot R^2 \cdot U_{wind}^3 \quad (1)$$

The Tip Speed Ratio  $\lambda$  is the ratio between the speed at the tip of the blade  $\omega \cdot R$  and the incident wind speed  $U_{wind}$ :

$$\lambda = \frac{\omega \cdot R}{U_{wind}} \quad (2)$$

The global efficiency  $\eta$  is calculated starting from the electric power  $P_{el}$  produced by the PMSG and the value of  $P_{wind}$ :

$$\eta = \frac{P_{el}}{P_{wind}} \quad (3)$$

The global efficiency can be partitioned in two contributions: the first parameter  $\eta_{el}$  is the electrical efficiency of the PMSG, while the second parameter  $C_{p,mech}$  is the coefficient of power, i.e., the ratio between the extracted mechanical power  $P_{mech}$  and  $P_{wind}$ .

$$\eta = C_{p,mech} \cdot \eta_{el} \quad (4)$$

$$C_{p,mech} = \frac{(P_{el} + P_{loss})}{P_{wind}} = \frac{P_{mech}}{P_{wind}} \quad (5)$$

For the sake of simplicity, the losses  $P_{loss}$  in the conversion of mechanical power into electrical power are partitioned into three contributions:

$$P_{loss} = P_{cop} + P_{iron} + P_{fric} \quad (6)$$

The copper losses  $P_{cop}$  are due to Joule effect in the armature windings of stator. They depend on the square of three-phase current in the stator windings and on the coils' resistance  $P_{cop}=3 \cdot R_{coils} \cdot I^2$ . The iron losses  $P_{iron}$  are a result of magnetic hysteresis and eddy currents. The friction losses  $P_{fric}$  are due to friction in the bearings.

At nominal conditions, the copper losses are  $P_{cop}=3 \cdot R \cdot I_{nom}^2$ , while both iron and friction losses are assumed equal to half of the copper losses:

$$P_{iron,nom} = P_{fric,nom} = 0.5 \cdot P_{cop,nom} \quad (7)$$

In operating conditions, the iron losses  $P_{iron}$  are considered proportional to the ratio between the measured voltage  $V$  and its nominal value  $V_{nom}$ :

$$P_{iron} = P_{iron,nom} \cdot \left(\frac{V}{V_{nom}}\right)^2 \quad (8)$$

The friction losses  $P_{fric}$  are proportional to the ratio between the angular speed  $\omega$  and its nominal value  $\omega_{nom}$ :

$$P_{fric} = P_{fric,nom} \cdot \left(\frac{\omega}{\omega_{nom}}\right)^2 \quad (9)$$

### III. INSTRUMENTATION AND MEASUREMENT CIRCUIT

The instrumentation, used to measure wind speed, rotor speed and electric parameters, is described below.

A hot wire anemometer (manufacturer: Lutron) is placed in front of the blade rotor in order to measure and set the desired wind speed  $U_{wind}$  (accuracy:  $\pm 5\%$  of reading).

An encoder is utilized to measure the speed of the rotor  $\omega$ .

A digital power meter (manufacturer: Yokogawa) is connected to the output of the PMSG in order to measure voltage  $V$ , phase current  $I$  and the generated power  $P_{out}$ , (typical uncertainties of  $\pm 0.1\%$ ,  $\pm 1\%$  and  $\pm 1.1\%$ , respectively).

Three variable resistances in star connection (with a maximum resistance of  $100 \Omega$ ) represent the load of the circuit. They are used to change the operating point of the system at constant wind speed. Fig. 2 shows the scheme of the electrical circuit.

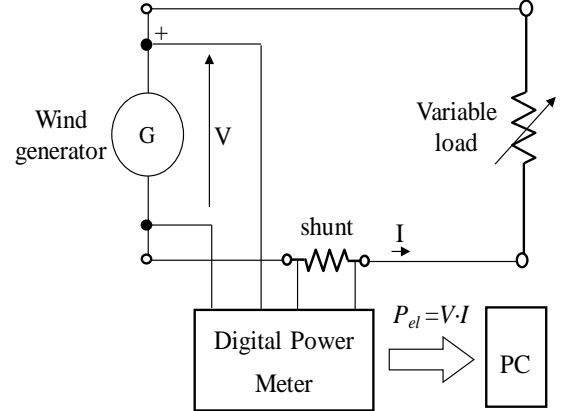


Fig. 2. Single-phase equivalent circuit of the test.

### IV. COMPONENTS OF THE SYSTEM

The first component of the generator is a 3D printed wind turbine, whose shape is optimized to better work at low wind speed. The airfoil is designed to reduce the Laminar Separation Bubbles (LSB) phenomena that result in excessive drag, inconsistent lift and noise [4].

The turbine is realized by a 3D printing procedure known as Fused Filament Fabrication [5]. It consists of the deposition of a stream of material, which immediately hardens to form a thin layer. A filament of thermoplastic is fed into an extrusion nozzle, which heats the material and apply it to the previous layer. For example, the nozzle moves upward in the working area and it creates

another layer, repeating the process until the object has built up. The micro wind-turbine is 3D printed by using polylactic acid (PLA), that is a biodegradable plastic derived from renewable resources, such as corn starch [6]. Its melting temperature is between 180 and 220°C and the density of the wire used to build the blade is 1.25 g/cm<sup>3</sup>. The weight of the prototype can vary with the infill density: in the case study, the wind turbine is realized with an infill density of 50% and the weight of a single blade is ≈70 g; the weight of the complete wind rotor is ≈470 g.

As shown in Fig. 3, the hub of the turbine is made to join the five blades and the other components; the nose is connected in the front, while the flange is fixed in the back. The external diameter of the hub is 60 mm and it is the best compromise between low aerodynamic interference and mechanical resistance. Five screws (ø 5 mm and length of 60 mm) are used to assemble the nose, the hub and the flange [7].

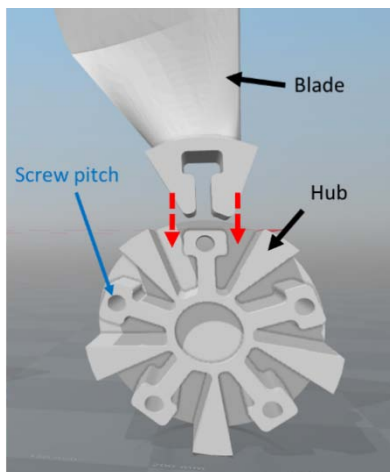


Fig. 3. Details of the mechanical connections

A permanent magnet generator is an electric machine in which the rotating magnetic field, as well as the inductor flux, is created by permanent magnets, instead of being originated by current passing through coils. These magnets are placed on the rotor. As well known, this rotating field can be generated also by windings placed in the stator slots, as in the case of asynchronous machine in Doubly Fed Induction Generator for wind power [8]. In the synchronous machine the frequency of the induced voltage in the stator is proportional to the angular speed of the rotor by the number of pole pairs. Since an external excitation circuit is missing in a PMSG, slip rings and contact brushes are avoided. A disadvantage is that the air gap flux cannot be controlled, so the voltage regulation is not easy.

The specifications of the PMSG used in the case study are shown in Table I. The wind tunnel used for the test is a closed return typology: a scheme of this type of tunnel is visible in Fig. 4.

Table I. Specifications of the PMSG

Torque (Nm)	1.271
Power output (W)	400
Speed (rpm)	3000
Current (A)	2.7
Max current (A)	8.1
Resistance (Ω)	4.7
Weight (kg)	5
Pole pairs	8

It consists of a series of air vanes and an open test section, where the prototype is installed. Air is moved by fans from the end of the test section back to it, passing by the vans. The test section of the wind tunnel used in this work has a diameter of 70 cm, which represents a limit for the size of the prototypes that can be tested. The length of test section is 1.75 m and the axis of the tunnel is placed at 1.1 m from the beginning. Turbulence effects are high due to important solid blockage that changes the velocity distribution as well as the coefficient of power. For the sake of simplicity, these effects are not considered in this work.

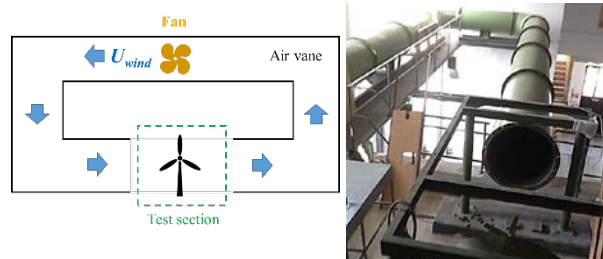


Fig. 4. The closed return wind tunnel

## V. RESULTS AND DISCUSSIONS

The most interesting results are the efficiency  $\eta$ - $\lambda$  curves for different wind conditions. In addition to the  $\eta$  diagram, the  $C_{p,mech}$  is shown in order to evaluate the losses due to the PMSG generator. The maximum value of  $\eta$  is ≈30%, while the  $C_{p,mech}$  reaches ≈40% with losses around 10%. Fig.5 shows the diagram of quantities  $\eta$  and  $C_{p,mech}$  obtained by the interpolation and the linear regression of the experimental data, corresponding to wind speeds in the range 9–13 m/s.

Fig. 6 shows the  $P_{mech}$ - $\omega$  curves in the abovementioned wind speed range. It is possible to notice that the locus of maximum power points is a cubic function of rotor speed  $\omega$  as the wind speed increases. The green line represents this locus of maximum power extracted from the wind turbine. With  $U_{wind}$ ≈8.7 m/s, the maximum power output is  $P_{el}$ ≈15 W and  $\omega$ ≈760 rpm; with  $U_{wind}$ =13 m/s, the maximum power  $P_{el}$ ≈68 W is extracted at  $\omega$ ≈1100 rpm.

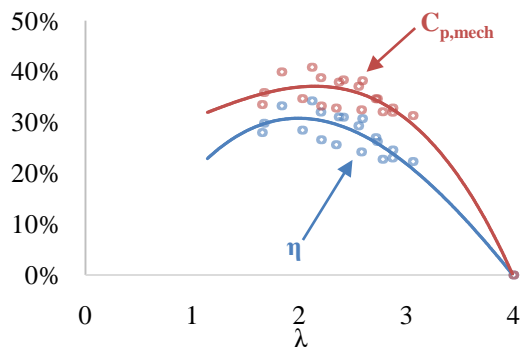


Fig. 5. The  $\eta$  and  $C_{p,mech}$  curves as a function of  $\lambda$

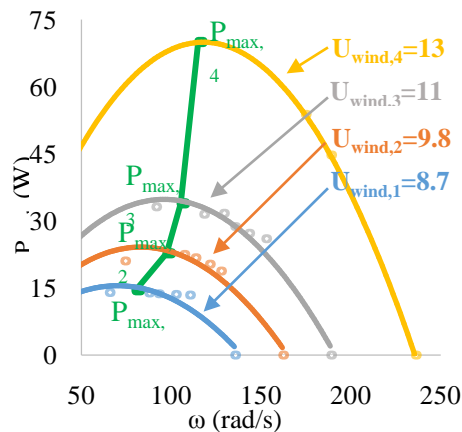


Fig. 6. The  $P_{mech}-\omega$  curves as a function of wind speed

The cut-in speed is higher than conventional values (around 4 m/s). It is due to the high weight of the wind rotor with respect to the size of the swept area. Thus, the system has a high inertia. At low wind speed, the turbine cannot win the resistive torque and does not start. There are different solutions: the first consists of the print of a bigger turbine with a higher swept area; otherwise, another electric generator should be used. On the contrary, in case of the realization of another turbine with a lower weight, the resistance to the centrifugal force and flexion could not be guaranteed. In a future work, the best compromise between the mechanical resistance of the material and the weight of the rotor will be investigated.

## VI. CONCLUSIONS AND FUTURE WORKS

This paper describes a procedure to test the performance of a micro wind turbine with horizontal-axis. A 3D printed prototype of turbine is connected to an electric generator and it is tested in a wind tunnel. Thanks to a set of variable resistance, the working point of the generator is varied and its performance is investigated at different wind speeds. In the case study, it is verified a fair performance of the tested turbine, directly coupled

with a PMSG. Actually, the maximum value of the system efficiency is  $\eta \approx 30\%$ .

Authors are working to apply the procedure to the rescaled rotor shown in Fig. 7 with a swept area of  $0.64 \text{ m}^2$  and  $P_{Betz} \approx 780 \text{ W}$  (at wind speed = 15 m/s). It will be installed in a bigger wind tunnel, with respect to that one used to test the procedure on the smaller prototype. The system will be upgraded by using torque meters: it will be possible to distinguish between mechanical and electric losses and verify the theoretical estimation of losses in the electric generator. The blades will be made studying the optimal compromise between the resistance to mechanical stress of materials and the total weight of the wind turbine. The goal is the reduction of the inertia and of the cut-in wind speed.



Fig. 7: 3D models of the five blades rotors

## REFERENCES

- [1] M.C.G. Carlos Fernandes, L. Blazquez, J. Sanesteban, R. C. Martins, Jorge H.O. Seabra, Energy efficiency tests in a full scale wind turbine gearbox, Tribology International, Volume 101, Sept. 2016, pp. 375-382.
- [2] R.P. Jerson. Vaz, H.David Wood, Performance analysis of wind turbines at low tip-speed ratio using the Betz-Goldstein model, Energy Conversion and Management, Volume 126, 15 Oct. 2016, pp. 662-672.
- [3] F. Spertino, J. Ahmad, G. Chicco, A. Ciocia and P. Di Leo, "Matching between electric generation and load: Hybrid PV-wind system and tertiary-sector users," 50th International Conference UPEC, 2015, pp. 1-6.
- [4] J. AlMutairi, E. ElJack, I. AlQadi, Dynamics of laminar separation bubble over NACA-0012 airfoil near stall conditions, Aerospace Science and Technology, vol 68, 2017, pp 193-203.
- [5] J. Go, S. N. Schiffres, A. G. Stevens, A. J. Hart, Rate limits of additive manufacturing by fused filament fabrication and guidelines for high-throughput system design, Additive Manufacturing, vol 16, 2017, pp 1-11.
- [6] Y. Song, Y. Li, W. Song, K. Yee, K.-Y. Lee, V.L. Tagarielli, Measurements of the mechanical response of unidirectional 3D-printed PLA, Materials & Design, vol 123, 2017, pp. 154-164.
- [7] J. F. Manwell, J. G. McGowan, A. L. Rogers, Wind Energy Explained: Theory, Design and Application, John Wiley & Sons Inc, 2009.
- [8] G. Chicco, P. Di Leo, F. Scapino and F. Spertino, "Experimental Analysis of Wind Farms connected to the High Voltage Grid: the Viewpoint of Power Quality," 2006 First International Symposium on Environment Identities and Mediterranean Area, Corte-Ajaccio, 2006, pp. 184-189.